

# Targeted Sub-threshold Search for Strongly-lensed Gravitational-wave Events

Alvin K. Y. Li,<sup>1, a</sup> Rico K. L. Lo,<sup>2, b</sup> Surabhi Sachdev,<sup>2, 3, 4</sup> Tjonnje G. F. Li,<sup>1</sup> and Alan J. Weinstein<sup>2</sup>

<sup>1</sup>*Department of Physics, The Chinese University of Hong Kong, Shatin, New Territories, Hong Kong*

<sup>2</sup>*LIGO Laboratory, California Institute of Technology, Pasadena, CA 91125, US*

<sup>3</sup>*Department of Physics, The Pennsylvania State University, University Park, PA 16802, USA*

<sup>4</sup>*Institute for Gravitation and the Cosmos, The Pennsylvania State University, University Park, PA 16802, USA*

(Dated: April 15, 2019)

Strong gravitational lensing of gravitational waves can produce duplicated signals that are separated in time and with different amplitudes. We consider the case in which strong lensing produces identifiable gravitational-wave events together with weaker sub-threshold signals that are hidden in the noise background. We present a search method for the sub-threshold signals using reduced template banks targeting specific confirmed gravitational-wave events. We apply the method to an event from Advanced LIGO's first observing run O1, GW151012. We show that the method is effective in reducing the noise background and hence raising the significance of (near-) sub-threshold triggers. In the case of GW151012, we are able to improve the sensitive distance by 10% – 25%. Finally, we present the 10 most significant events for GW151012-like signals in O1. Besides the already confirmed gravitational-wave detections, none of the candidates pass our nominal significance threshold of False-Alarm-Rate  $\leq 1/30$  days.

## I. INTRODUCTION

The LIGO-Virgo Collaboration [1–4] has successfully made 11 confident detections of gravitational waves from compact binary mergers [5] as of the time of writing, which have verified the existence of gravitational waves predicted by Albert Einstein's general theory of relativity [6]. The study of gravitational waves has been applied to many different aspects of physics, including multi-messenger astronomy [7–12], cosmology [13–15], testing general relativity [16, 17] and even particle physics [18, 19].

General relativity also predicts that, as masses can curve spacetime, waves emitted from a source can be bent and deflected before reaching the observer, an effect known as *gravitational lensing*. This effect has been extensively studied in the context of electromagnetic waves over the last century [20–26]. Recent work have started considering gravitational lensing of gravitational waves, including the rate of lensing [27–31], the effects of strong lensing on gravitational-wave waveforms [32–39], and weak lensing effects imprinted onto the gravitational waveforms [40, 41]. A recent study has shown, however, that there was no strong evidence for the observation of gravitational lensing during the first observing run (O1) and the second observing run (O2) [27]. Nevertheless, with the expected rise in the detection rate of gravitational waves from binary black hole mergers in the coming years [42], there is a chance that we will observe lensed gravitational-wave signals.

Under the influence of strong gravitational lensing, multiple signals from the same source can arrive with relative time delay and magnification. Therefore, it is possible to have gravitational-wave signals with sufficiently strong amplitudes that can be identified as detections and corresponding weaker gravitational-wave signals which are buried in the noise background. We refer to these weaker signals as *sub-threshold*.

In this paper, we present a search for sub-threshold lensed signals using information from confirmed gravitational-wave events. In particular, we use information from detected events to limit the parameter space for our matched-filtering analysis. Similar analyses have been developed to target gamma-ray bursts (GRBs) [43] and sub-solar mass compact binaries [44]. For example, Ref. [43] made use of confirmed gamma-ray burst signals to fix the time and sky location for the search of the associated gravitational waves and showed an improvement of 25% in terms of the sensitive distance.

The paper is outlined as follows. Sec. II provides an overview of the proposed method. In Sec. III we describe the results of this analysis on a gravitational-wave event, namely GW151012. Finally, we give the conclusions and discuss the future improvements in Sec. IV.

## II. METHODS

Before describing the targeted sub-threshold search method for strongly-lensed gravitational-wave signals in detail, we first give an overview of the search (see Fig. 1).

Suppose we want to search for strongly-lensed counterparts of a gravitational-wave event, which are potentially sub-threshold because of the *relative de-magnification*. This means the counterparts will appear to be further away from the observing point and hence the signals will be weaker. As an input to the search, a number of posterior samples of parameters obtained from parameter estimation (e.g. from LALInference [45]) of the event of interest are used to generate a set of injections<sup>1</sup>. For each posterior sample selected, we generate one injection with its original strength, and nine additional weaker injections to mimic its weaker lensed counterparts.

<sup>a</sup> alvin.li@ligo.org

<sup>b</sup> kll@caltech.edu

<sup>1</sup> An injection refers to a simulated lensed signal that we test a search pipeline against to measure the effectiveness of the pipeline

After obtaining an injection set, we run a matched-filtering based search pipeline to see what templates in the full template bank can recover these injected signals with *sufficiently high* significance. In this work, we are applying the `GstLAL` pipeline [46, 47]. In principle, the search will work equally well for any other matched-filtering based pipelines such as `PyCBC`[48]. These templates will then be used to form the *reduced template bank* to search for the sub-threshold lensed signals. Detailed description of the generation of the reduced template bank can be found in Section II A.

We then use the same search pipeline to perform a search, with the identical procedures as the usual analyses but with our newly obtained reduced template bank, whose size is much smaller than the original bank, to look for candidates of strongly-lensed counterparts from all the available data.

Compared to a search using the full template bank, a weaker lensed signal of the event of interest will have a higher statistical significance in a search using the smaller reduced template bank because of the reduction in the trial factor. Further explanation can be found in section II B.

As an output of the search, we give a list of possible strongly-lensed signals of the targeted gravitational-wave event. These triggers will then be followed-up using a Bayesian model selection analysis. The follow-up analysis is described in another upcoming paper [49]. The interpretation of the statistical significance of these triggers is described in Section II B.

### A. Reduced template bank

Our starting point is the template bank used for Advanced LIGO's observing run O2, with the parameter space of masses of the binary components spanning from  $2M_{\odot}$  to  $400M_{\odot}$ , covering binary neutron stars (BNS), neutron-star-black-hole (NSBH) and binary black hole (BBH) systems, with a total of 677000 templates [47, 50]. For templates dedicated for BBH systems, they carry (anti-)aligned dimensionless spin magnitudes  $\leq 0.999$ . This spin limit is chosen to be as close to the theoretical limit of 1 as possible with current waveform approximants.

To generate a reduced template bank that is effectual in identifying lensed signals of the event of interest, we need to figure out what templates in the original template bank are able to find these weaker signals. To achieve this, we perform an injection campaign where simulated lensed signals are injected into the data.

Since the parameters (e.g. masses and spins) of a gravitational-wave signal are not exactly known, we use the posterior samples of  $N_{\text{ps}} = \mathcal{O}(1000)$  highest likelihood values from parameter estimation to represent the event. For a matched-filtering based CBC search, the templates are characterized by the intrinsic parameters, such as component masses and spins, since they govern the evolution of a waveform over time. The dependence on other extrinsic parameters, such as luminosity distance  $D_L$  and inclination  $\iota$ , are absorbed into

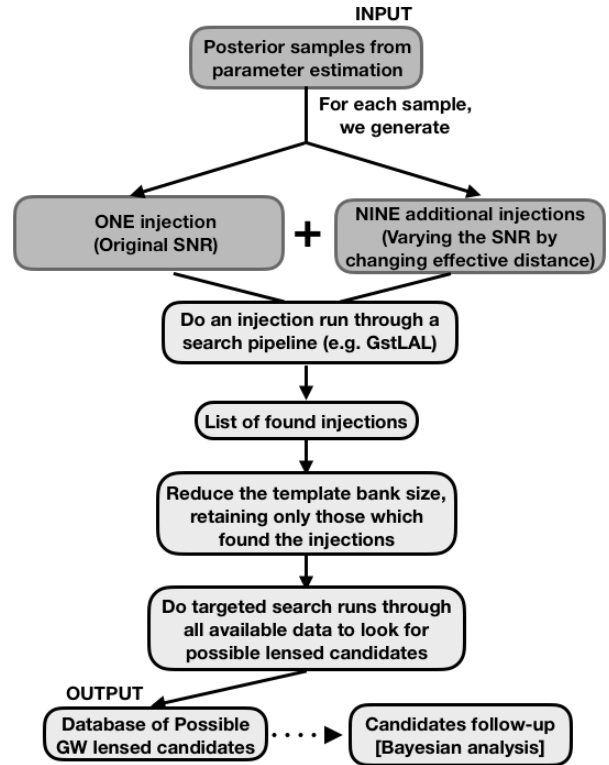


Figure 1. The flow-chart outlining briefly the workflow of the targeted sub-threshold search method. We will describe each step in detail in Section II.

the effective distance  $D_{\text{eff}}$ , which is defined in [51] as

$$D_{\text{eff}} = D_L \left[ F_+^2 \left( \frac{1 + \cos^2 \iota}{2} \right) + F_{\times}^2 \cos^2 \iota \right]^{-1/2}, \quad (1)$$

where  $F_+$  and  $F_{\times}$  are the antenna pattern of a GW detector to the plus and cross polarization of GW respectively. The optimal SNR  $\rho_{\text{opt}} = \sqrt{\langle h|h \rangle}$  of a template  $h_{\text{template}}$  is given by

$$\rho_{\text{opt}}^2 = \langle h|h \rangle = 4 \int_0^{\infty} df \frac{|h_{\text{template}}|^2}{S_n(f)} \propto \left( \frac{1}{D_{\text{eff}}} \right)^2, \quad (2)$$

where  $S_n(f)$  is the one-sided power spectrum density of the noise in a detector [51]. Each template in a template bank is *normalized by the optimal SNR squared* such that the matched-filtering SNR is independent of the strength of the templates. The signal-to-noise (SNR) ratio  $\rho_{\text{opt}}$  then scales with the effective distance as

$$\rho_{\text{opt}} \propto \frac{1}{D_{\text{eff}}}. \quad (3)$$

For each posterior sample, we make one injection with the original optimal SNR, and nine additional injections with

smaller optimal SNRs by varying their *effective distances* to mimic the weaker lensed images of the event of interest, since the optimal SNR scales with  $1/D_{\text{eff}}$  as in Eq. 3. After generating a set of  $10N_{\text{ps}}$  injections, we inject these simulated lensed signals into the data, and use a matched-filtering based CBC search pipeline (such as `GstLAL`) to try recovering the injected signals. An injection is said to be found if the corresponding trigger<sup>2</sup> has a *False-Alarm-Rate (FAR) of less than 1 per 30 days*. The templates that recovered the injections will be put into the reduced template bank for the sub-threshold search. Doing the injection campaign described above makes sure that the templates in the reduced template bank will be able to identify the sub-threshold lensed signals, if they truly exist in the data.

### B. Statistical significance of triggers

Each gravitational-wave candidate in `GstLAL` search is assigned a likelihood-ratio statistic  $\mathcal{L}$  [46, 47, 52, 53] to measure its significance. The likelihood-ratio is assigned based on the SNR, a signal consistency check (`GstLAL` uses the normalized power in the difference of the SNR time series and the autocorrelation time series), the sensitivity of each detector at the time of the candidate, and the time and phase delays between the triggers from different detectors. A p-value or False-Alarm-Probability (FAP) is then calculated for each event. False-Alarm-Probability is the probability that noise would produce a trigger with a ranking statistic  $\ln \mathcal{L}$  greater or equal to the ranking statistic  $\ln \mathcal{L}^*$  of the trigger under consideration. In case of a single event, in terms of  $\ln \mathcal{L}$ , it is just the complementary cumulative distribution function of the likelihood-ratio,

$$P(\ln \mathcal{L} \geq \ln \mathcal{L}^* \mid \text{noise}) = \int_{\ln \mathcal{L}^*}^{\infty} P(\ln \mathcal{L} \mid \text{noise}) d \ln \mathcal{L}. \quad (4)$$

In case of  $M$  observed events, the FAP becomes,

$$\begin{aligned} &P(\ln \mathcal{L} \geq \ln \mathcal{L}^* \mid \text{noise}_1, \dots, \text{noise}_M) \\ &= 1 - (1 - P(\ln \mathcal{L} \geq \ln \mathcal{L}^* \mid \text{noise}))^M. \end{aligned} \quad (5)$$

Alternatively, we can express an event's significance in terms of the False-Alarm-Rate, which refers to how often noise would produce a trigger with ranking statistic  $\ln \mathcal{L}$  greater or equal to the ranking statistic  $\ln \mathcal{L}^*$  of the trigger under consideration [46]. In terms of the complementary cumulative distribution function of the likelihood-ratio and the time length of the data under analysis  $T$ ,

$$\text{FAR} = \frac{P(\ln \mathcal{L} \geq \ln \mathcal{L}^* \mid \text{noise})}{T}. \quad (6)$$

As we have briefly discussed before in Section I, we expect to increase the significance of sub-threshold triggers by

reducing the size of a template bank. By targeting a subset of the parameter space, we can increase the significance of events present in the reduced subspace by reducing the trial factors. Since we are only interested in signals that belong to that subspace, the foreground is kept constant while the background is lowered. This method has the potential to reveal sub-threshold signals belonging to a restricted parameter space, and can be used to look for quieter lensed counterparts of the gravitational-wave signals detected by LIGO-Virgo.

When we make use of the reduced template bank for the targeted search of lensed companions of the targeted GW event, the `GstLAL` pipeline associates each found trigger a False-Alarm-Probability FAP and a False-Alarm-Rate FAR (See Table II as an example). Readers should be reminded that the FAPs evaluated here are not indicators of how likely/unlikely the triggers are lensed counterparts of the targeted event, since the FAP evaluated here is only indicating how likely the identified trigger is a gravitational-wave signal. Instead, the output of this search should only be interpreted as a priority list for follow-up analysis that computes the likelihood that two triggers share the same set of source parameters. This means, we need a further analysis for the triggers obtained from the search which also evaluates the likelihood that they are lensed gravitational-wave signals from the same source (i.e. the target event). The Bayesian model selection between lensed and unlensed hypotheses will be explored in a follow-up paper [49].

## III. SEARCHING FOR SUB-THRESHOLD GRAVITATIONAL WAVES ASSOCIATED WITH GW151012

### A. Constructing the Reduced Template Bank

To study the performance of our proposed method, we apply it to the gravitational-wave event GW151012 [5, 54]. GW151012 represents the case where the initial detection is considered marginal. Table I summarises the information about GW151012.

Properties	Value
UTC time	Oct 12 2015 09:54:43.44
GPS time	1128678900.44
Primary mass in source frame $m_1^{\text{source}}$	$23_{-6}^{+18} M_{\odot}$
Secondary mass in source frame $m_2^{\text{source}}$	$13_{-5}^{+4} M_{\odot}$
Chirp mass in source frame $\mathcal{M}_c^{\text{source}}$	$15.1_{-1.1}^{+1.4} M_{\odot}$
Luminosity distance $D_L$	$1000_{-500}^{+500}$ Mpc
Source redshift $z$	$0.20_{-0.09}^{+0.09}$
Signal-to-noise ratio $\rho$	9.7
False-Alarm-Rate FAR	$0.37 \text{ yr}^{-1}$

Table I. Essential information of the gravitational-wave event GW151012 reported in [54].

We generate the reduced template bank by first selecting posterior samples with aligned spins released by the LIGO-Virgo collaboration [55]. We use these samples to simulate 25524 lensed signals with varying strengths (or equivalently

<sup>2</sup> That is the time of trigger is within a certain window of the injected time.

at varying effective distances) in the time near GW151012. Figure 2 shows the distribution of injections in the chirp mass (detector frame)  $\mathcal{M}_c^{\text{detector}}$  - effective spin  $\chi_{\text{eff}}$  parameter space. The orange cross indicates the median inferred value for  $\mathcal{M}_c^{\text{detector}}$  and  $\chi_{\text{eff}}$  reported in Ref. [54]. We confirm that the injections mainly populate around the median inferred value.

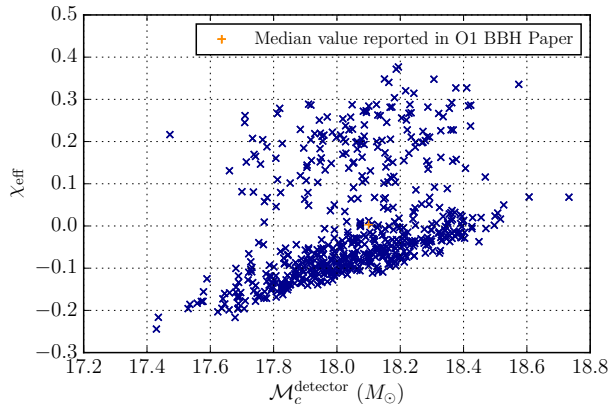


Figure 2. The injection set used in the injection campaign for the GW151012 targeted search in the chirp mass in detector frame  $\mathcal{M}_c^{\text{detector}}$  - effective spin parameter  $\chi_{\text{eff}}$  plane. The orange cross indicates the median inferred value for the chirp mass in detector frame and the effective spin parameters for GW151012 reported in [54].

The templates which successfully (i.e.  $\text{FAR} \leq 1/30$  days) identify our injected signals are added to the reduced template bank. Figure 3 shows the original template bank (dark blue) used by the `GstLAL` search in observing runs O1 and O2, and the reduced template bank (orange) generated for the sub-threshold search of GW151012 projected onto an  $m_1 - m_2$  plane. We can see that the reduced template bank is more sparse than the original bank. In fact, there are only 1063 templates in the reduced template bank, while there are 677000 templates in the full template bank. Note that there is a fraction of low-mass templates in our reduced template bank in Fig. 3. We believe that these are caused by noise fluctuations for triggers with significance close to the threshold. We are aware of these nonphysical templates and we will further improve our method to remove these templates, one being implementing a suitable black hole mass distribution into the likelihood calculation in the search pipeline[56].

To confirm that our reduced template bank is effectual and improves sensitivity, we use the reduced template bank to analyse the same set of injections and data as above. Figure 4 shows the comparison plot of the False-Alarm-Rate (FAR) for the found injected simulated lensed signals of GW151012 by using the original and reduced template bank. For injections near the usual threshold for FAR (i.e.  $\text{FAR} \approx 10^{-7}$ Hz), it can be seen that most injections have their FAR lowered through the use of the reduced template bank. Overall, out of 1555 recovered injections, the FAR of 755 (48%) injections have been lowered. This shows that the use of a reduced template bank can effectively reduce the noise background, and hence

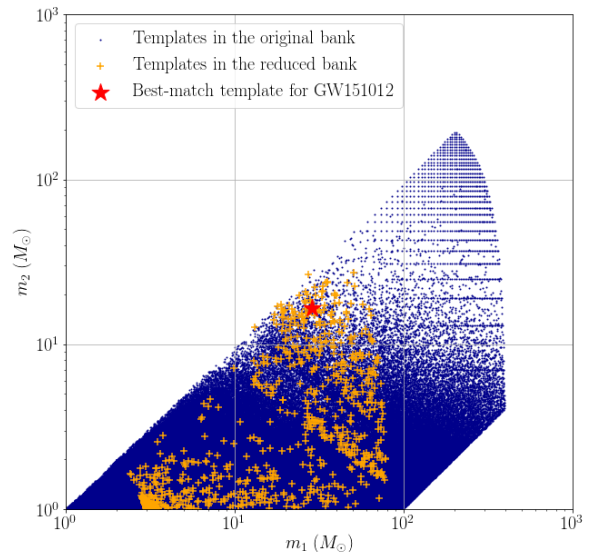


Figure 3. (Color online) The templates in the original and the reduced template bank, plotted in dark blue and orange respectively on the  $m_1 - m_2$  plane. The best-match template for GW151012 is indicated by a red star. We can see that the reduced template bank is more sparse than the original bank. However, because the templates in the reduced template bank can recover the lensed signal injections in an injection campaign, these templates will be able to identify the sub-threshold lensed signals, if they truly exist in the data.

improving the ranking statistics (which, in this case, is lowering the FAR) of (near-) sub-threshold signals.

## B. Search Sensitivity

To assess the search sensitivity of our targeted search, we analyse the same injection set as above but now in the full data from O1 using the original and reduced template bank. Figure 5 compares the distribution of ranking statistic ( $\log$  likelihood  $\ln \mathcal{L}$ ). Note that the blue curve (with reduced template bank) is below the red curve (with original bank), indicating that the noise background is reduced when we use the reduced template bank.

From our set of injections with known distances, we can assess the distance out to which we may be able to identify gravitational-wave events (observable range). Figure 6 shows the observable range - FAR curves for GW151012-like signals using the original and reduced template bank. Note that the orange curve (with reduced template bank) is shifted upward compared to the blue curve (using the full template bank), indicating an increase in the observable range. In fact, the observable range is improved by at least 10%. In particular, around the usual threshold for the False-Alarm-Rate FAR (i.e.  $\text{FAR} \approx 10^{-7}$ Hz), the observable range is improved by approximately 25%. This suggests that with the use of a re-

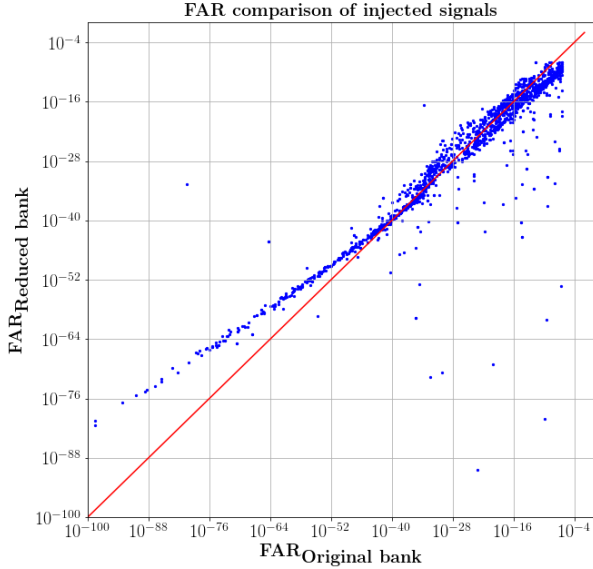


Figure 4. The comparison plot of the False-Alarm-Rate (FAR) for the found injected simulated lensed signals of GW151012 by using the original and reduced template bank. The red line indicates the identity line. For injections near the usual threshold value for FAR (i.e.  $\text{FAR} \approx 10^{-7} \text{Hz}$ ), most injections have their FAR lowered through the use of the reduced template bank. The plot shows in total 1555 recovered injections, and 755 injections (48%) have their FAR reduced through the use of the reduced template bank. This means that the use of a reduced template bank effectively raises the ranking significance (FAR) of (near-) sub-threshold triggers

duced template bank, we are able to see gravitational-wave signals from further distance with the same FAR threshold. From Eq. 3 we can conclude that we are able to improve the ranking statistics of signals with weaker amplitudes by the use of a targeted reduce template bank.

### C. Strong-lensing Candidates of GW151012

Finally, we present the list of the top 10 candidates of strongly-lensed images of GW151012 identified by this search over all data from observing run O1 in Table II. A number of items should be noted. As we can see, our reduced template bank retrieved all the three confirmed gravitational-wave events from observing run O1 (in ascending order of FARs: GW150914, GW151012, GW151226). However, the False-Alarm-Rate (FAR) for the events GW150914 and GW151226 increased when using reduced template bank, while that for GW151012 decreased. This result is expected because we are creating the reduced template bank dedicated for the search of lensed counterparts of GW151012, and hence some of the original templates that match the other two events GW150914 and GW151226 well are eliminated through the injection campaign and in turn reducing their significance. On the other hand, we are keeping those templates that match GW151012

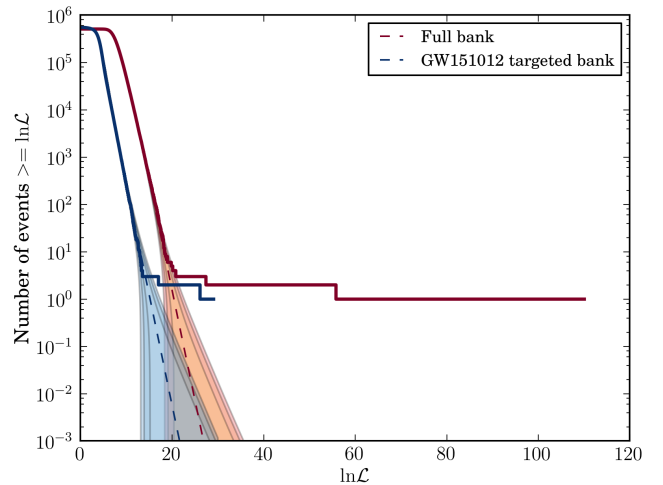


Figure 5. (Colour online) The ranking statistic threshold curves (on the log likelihood  $\ln \mathcal{L}$  - Number of events  $N > \ln \mathcal{L}$  plane) for GW151012. Note that the results combined all the data in the observing run O1. The red curve corresponds to the result using the original full template bank, while the blue curve corresponds to the result using the reduced template bank. It should be noted that the blue curve is below the red one, indicating that the noise background has been reduced through reducing the template bank size.

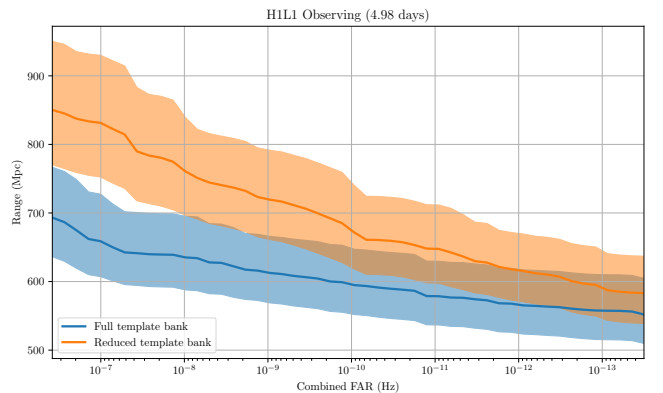


Figure 6. (Colour online) The observable range - combined False-Alarm-Rate (FAR) plots for GW151012 using the original and reduced template bank. The curve with the reduced template bank is above the one with the original full template bank. In general the improvement in observable range is at least 10%. Particularly, around the usual threshold for FAR (i.e.  $\text{FAR} \approx 10^{-7} \text{Hz}$ ), the observable range is improved by approximately 25%.

(and its lensed counterparts) and therefore we increase the significance of GW151012.

However, with the usual FAR threshold (i.e.  $\text{FAR} \leq 1/30$  days), none of the other triggers from Table II passes the threshold. This means that we have not identified any lensed counterparts for GW151012 in the data from observing run O1. Nevertheless, readers should be reminded that the FAR shown on Table II do not indicate how likely these triggers are lensed counterparts of the targeted gravitational-wave event, but instead a priority ranking for follow-up analysis that

Rank	GPS Time	UTC Time	SNR	$\text{FAR}_{\text{full bank}} \text{ (Hz)}$	$\text{FAR}_{\text{reduced bank}} \text{ (Hz)}$	Remark
1	1126259462.42	Sep 14 2015 09:50:45.42	18.71	$1.577 \times 10^{-47}$	$9.21 \times 10^{-14}$	This is GW150914
2	1128678900.44	Oct 12 2015 09:54:43.44	10.03	$1.385 \times 10^{-10}$	$2.12 \times 10^{-12}$	This is GW151012
3	1135136350.66	Dec 26 2015 03:38:53.66	9.88	$1.287 \times 10^{-23}$	$2.06 \times 10^{-8}$	This is GW151226
4	1128146827.56	Oct 06 2015 06:06:50.56	8.75	$2.908 \times 10^{-6}$	$1.16 \times 10^{-6}$	
5	1135879197.13	Jan 03 2016 17:59:40.13	8.36	-	$1.49 \times 10^{-6}$	This trigger was not found in the full bank search.
6	1133747525.57	Dec 10 2015 01:51:48.57	8.61	$7.662 \times 10^{-5}$	$1.63 \times 10^{-6}$	
7	1127655127.23	Sep 30 2015 13:31:50.23	8.75	$9.828 \times 10^{-5}$	$1.68 \times 10^{-6}$	
8	1126595209.37	Sep 18 2015 07:06:32.37	11.66	$3.582 \times 10^{-5}$	$1.93 \times 10^{-6}$	
9	1127408321.32	Sep 27 2015 16:58:24.32	8.30	-	$2.17 \times 10^{-6}$	This trigger was not found in the full bank search.
10	1127483108.22	Sep 28 2015 13:44:51.22	8.56	-	$2.24 \times 10^{-6}$	This trigger was not found in the full bank search.

Table II. A list of top 10 candidates of strongly-lensed images of GW151012 found by this search over all the O1 data.

computes the likelihood that two triggers share the same set of source parameters.

#### IV. CONCLUDING REMARKS

Gravitational-wave lensing has been the focus of increased attention in the recent literature [28–41]. A recent study has found no compelling evidence for lensing magnification, repeated signals from a single strongly lensed source, and wave optics effects due to solar-mass compact objects [27] in the GWTC-1 catalog [5]. Nevertheless, the possibility exists that strong lensing produces strong signals that can be identified as a gravitational-wave event and weaker signals that are buried inside the noise background. The latter are referred to as sub-threshold and may not be labelled as a gravitational-wave detection without further analysis.

We have proposed a search for these sub-threshold signals by means of matched-filtering using a reduced template bank that is produced to target specific gravitational-wave events. In particular, we construct this targeted template bank by selecting high-likelihood samples from the parameter estimation results, simulating a set of signals with varying distances from these samples and selecting the templates that successfully detect these signals. We show that the resulting reduced template bank reduces the noise background and increase the search sensitivity. Applied to an event from the Advanced LIGO’s first observing run O1, GW151012, we found that the sensitive distance increases by 10% – 25%.

We also present the list of triggers with the lowest False-Alarm-Rates for both targeted searches. With the usual FAR threshold (i.e.  $\text{FAR} \leq 1/30$  days), then it can be concluded that we have found no sub-threshold lensed signals for GW151012 in the data from observing run O1. Nevertheless, it should be noted that our reduced bank successfully lowers the noise background, and hence increases the significance of the (near-) sub-threshold triggers.

The new False-Alarm-Probability associated with these triggers should not be interpreted as a measure of the likelihood that these triggers are indeed duplicated signals of the same source. Instead, the output of this search should be interpreted as a priority list for follow-up analysis that computes the likelihood that two triggers share the same set of source

parameters [29, 49].

The performance of our search can be further optimized. For example, the selection procedure for templates that are included in the reduced bank may require tuning to find the optimal balance between coverage and sensitivity. Moreover, it has been shown that the subdivision of templates within a bank can also affect the performance. Furthermore, since we are looking for lensed counterparts of targeted events, from the sky location of the target, we should be able to set a consistent range for the difference in arrival time between the detectors for the lensed counterparts. With such, we can further increase the sensitivity of the search.

#### ACKNOWLEDGMENTS

The authors acknowledge the generous support from the National Science Foundation in the United States. The authors would also like to acknowledge Jonah Kanner for his useful suggestion. RKLL and TGFL would also like to gratefully acknowledge the support from the Croucher Foundation in Hong Kong. The work described in this paper was partially supported by a grant from the Research Grants Council of the Hong Kong (Project No. CUHK 14306218) and the Direct Grant for Research from the Research Committee of the Chinese University of Hong Kong. SS was supported in part by the LIGO Laboratory and in part by the Eberly Research Funds of Penn State, The Pennsylvania State University, University Park, PA 16802, USA.

The authors are also grateful for computational resources provided by the LIGO Laboratory and supported by National Science Foundation Grants PHY-0757058 and PHY-0823459. This research has made use of data, software and/or web tools obtained from the Gravitational Wave Open Science Center (<https://www.gw-openscience.org>) [57], a service of LIGO Laboratory, the LIGO Scientific Collaboration and the Virgo Collaboration. LIGO was constructed by the California Institute of Technology and Massachusetts Institute of Technology with funding from the National Science Foundation and operates under cooperative agreement PHY-0757058. Virgo is funded by the French Centre National de Recherche Scientifique (CNRS), the Italian Istituto Nazionale della Fisica Nucleare (INFN) and the Dutch Nikhef, with contributions

- [1] J. Aasi *et al.* (LIGO Scientific), *Class. Quant. Grav.* **32**, 074001 (2015), arXiv:1411.4547 [gr-qc].
- [2] B. P. Abbott *et al.* (KAGRA, LIGO Scientific, VIRGO), *Living Rev. Rel.* **21**, 3 (2018), arXiv:1304.0670 [gr-qc].
- [3] G. M. Harry (LIGO Scientific), *Gravitational waves. Proceedings, 8th Edoardo Amaldi Conference, Amaldi 8, New York, USA, June 22-26, 2009*, *Class. Quant. Grav.* **27**, 084006 (2010).
- [4] F. Acernese *et al.* (VIRGO), *Class. Quant. Grav.* **32**, 024001 (2015), arXiv:1408.3978 [gr-qc].
- [5] B. P. Abbott *et al.* (LIGO Scientific, Virgo), (2018), arXiv:1811.12907 [astro-ph.HE].
- [6] A. Einstein and M. Grossmann, *Zeitschrift für Mathematik und Physik* **63** (1914).
- [7] B. P. Abbott *et al.* (LIGO Scientific, Virgo, Fermi GBM, INTEGRAL, IceCube, AstroSat Cadmium Zinc Telluride Imager Team, IPN, Insight-Hxmt, ANTARES, Swift, AGILE Team, 1M2H Team, Dark Energy Camera GW-EM, DES, DLT40, GRAWITA, Fermi-LAT, ATCA, ASKAP, Las Cumbres Observatory Group, OzGrav, DWF (Deeper Wider Faster Program), AST3, CAASTRO, VINROUGE, MASTER, J-GEM, GROWTH, JAGWAR, CaltechNRAO, TTU-NRAO, NuSTAR, Pan-STARRS, MAXI Team, TZAC Consortium, KU, Nordic Optical Telescope, ePESSTO, GROND, Texas Tech University, SALT Group, TOROS, BOOTES, MWA, CALET, IKI-GW Follow-up, H.E.S.S., LOFAR, LWA, HAWC, Pierre Auger, ALMA, Euro VLBI Team, Pi of Sky, Chandra Team at McGill University, DFN, ATLAS Telescopes, High Time Resolution Universe Survey, RIMAS, RATIR, SKA South Africa/MeerKAT), *Astrophys. J.* **848**, L12 (2017), arXiv:1710.05833 [astro-ph.HE].
- [8] B. P. Abbott *et al.* (LIGO Scientific, Virgo, Fermi-GBM, INTEGRAL), *Astrophys. J.* **848**, L13 (2017), arXiv:1710.05834 [astro-ph.HE].
- [9] E. Burns *et al.* (Fermi Gamma-ray Burst Monitor Team, LIGO Scientific, Virgo), (2018), arXiv:1810.02764 [astro-ph.HE].
- [10] B. P. Abbott *et al.* (LIGO Scientific, Virgo), *Phys. Rev.* **D94**, 102001 (2016), arXiv:1605.01785 [gr-qc].
- [11] J. Aasi *et al.* (LIGO Scientific, VIRGO), *Astrophys. J. Suppl.* **211**, 7 (2014), arXiv:1310.2314 [astro-ph.IM].
- [12] B. P. Abbott *et al.* (LIGO Scientific, Virgo), (2019), arXiv:1901.03310 [astro-ph.HE].
- [13] B. P. Abbott *et al.* (LIGO Scientific, Virgo, 1M2H, Dark Energy Camera GW-E, DES, DLT40, Las Cumbres Observatory, VINROUGE, MASTER), *Nature* **551**, 85 (2017), arXiv:1710.05835 [astro-ph.CO].
- [14] B. P. Abbott *et al.* (LIGO Scientific, Virgo), *Phys. Rev. Lett.* **121**, 161101 (2018), arXiv:1805.11581 [gr-qc].
- [15] J. Aasi *et al.* (LIGO Scientific, VIRGO), *Phys. Rev. Lett.* **112**, 131101 (2014), arXiv:1310.2384 [gr-qc].
- [16] B. P. Abbott *et al.* (LIGO Scientific, Virgo), *Phys. Rev. Lett.* **116**, 221101 (2016), [Erratum: *Phys. Rev. Lett.* **121**, no. 12, 129902 (2018)], arXiv:1602.03841 [gr-qc].
- [17] B. P. Abbott *et al.* (LIGO Scientific, Virgo), (2018), arXiv:1811.00364 [gr-qc].
- [18] A. Albert *et al.* (ANTARES, IceCube, Pierre Auger, LIGO Scientific, Virgo), *Astrophys. J.* **850**, L35 (2017), arXiv:1710.05839 [astro-ph.HE].
- [19] S. Adrian-Martinez *et al.* (ANTARES, IceCube, LIGO Scientific, Virgo), *Phys. Rev.* **D93**, 122010 (2016), arXiv:1602.05411 [astro-ph.HE].
- [20] S. Rahvar and J. W. Moffat, *Mon. Not. Roy. Astron. Soc.* **482**, 4514 (2019), arXiv:1807.07424 [gr-qc].
- [21] P. V. P. Cunha and C. A. R. Herdeiro, *Gen. Rel. Grav.* **50**, 42 (2018), arXiv:1801.00860 [gr-qc].
- [22] S. G. Turyshev and V. T. Toth, *Phys. Rev.* **D96**, 024008 (2017), arXiv:1704.06824 [gr-qc].
- [23] V. I. Dokuchaev and N. O. Nazarova, *JETP Lett.* **106**, 637 (2017), [*Pisma Zh. Eksp. Teor. Fiz.* **106**, no. 10, 609 (2017)], arXiv:1802.00817 [astro-ph.HE].
- [24] M. Bartelmann and M. Maturi (2016) arXiv:1612.06535 [astro-ph.CO].
- [25] R. Narayan and M. Bartelmann, in *13th Jerusalem Winter School in Theoretical Physics: Formation of Structure in the Universe Jerusalem, Israel, 27 December 1995 - 5 January 1996* (1996) arXiv:astro-ph/9606001 [astro-ph].
- [26] R. B. Metcalf *et al.*, (2018), arXiv:1802.03609 [astro-ph.GA].
- [27] O. A. Hannuksela, K. Haris, K. K. Y. Ng, S. Kumar, A. K. Mehta, D. Keitel, T. G. F. Li, and P. Ajith, (2019), arXiv:1901.02674 [gr-qc].
- [28] M. Oguri, (2018), 10.1093/mnras/sty2145, arXiv:1807.02584 [astro-ph.CO].
- [29] K. Haris, A. K. Mehta, S. Kumar, T. Venumadhav, and P. Ajith, (2018), arXiv:1807.07062 [gr-qc].
- [30] K. K. Y. Ng, K. W. K. Wong, T. Broadhurst, and T. G. F. Li, *Phys. Rev.* **D97**, 023012 (2018), arXiv:1703.06319 [astro-ph.CO].
- [31] G. P. Smith, M. Jauzac, J. Veitch, W. M. Farr, R. Massey, and J. Richard, *Mon. Not. Roy. Astron. Soc.* **475**, 3823 (2018), arXiv:1707.03412 [astro-ph.HE].
- [32] G. P. Smith *et al.*, *Proceedings, IAU Symposium 338: Gravitational Wave Astrophysics: Early Results from GW Searches and Electromagnetic Counterparts: Baton Rouge, LA, USA, October 16-19, 2017*, *IAU Symp.* **338**, 98 (2017), arXiv:1803.07851 [astro-ph.CO].
- [33] P. Cremonese and E. Mrtzell, (2018), arXiv:1808.05886 [astro-ph.HE].
- [34] A. Pirkowska, M. Biesiada, and Z.-H. Zhu, *JCAP* **1310**, 022 (2013), arXiv:1309.5731 [astro-ph.CO].
- [35] R. Takahashi, *Astrophys. J.* **835**, 103 (2017), arXiv:1606.00458 [astro-ph.CO].
- [36] M. Sereno, A. Sesana, A. Bleuler, P. Jetzer, M. Volonteri, and M. C. Begelman, *Phys. Rev. Lett.* **105**, 251101 (2010), arXiv:1011.5238 [astro-ph.CO].
- [37] T. G. F. Li, *Extracting Physics from Gravitational Waves* (Springer International Publishing, 2015).
- [38] K.-H. Lai, O. A. Hannuksela, A. Herrera-Martín, J. M. Diego, T. Broadhurst, and T. G. F. Li, *Phys. Rev.* **D98**, 083005 (2018), arXiv:1801.07840 [gr-qc].
- [39] A. J. Moylan, D. E. McClelland, S. M. Scott, A. C. Searle, and G. V. Bicknell, in *Recent developments in theoretical and experimental general relativity, gravitation and relativistic field theories. Proceedings, 11th Marcel Grossmann Meeting, MG11, Berlin, Germany, July 23-29, 2006. Pt. A-C* (2007) pp. 807–823, arXiv:0710.3140 [gr-qc].
- [40] Y. Wang, A. Stebbins, and E. L. Turner, *Phys. Rev. Lett.* **77**, 2875 (1996), arXiv:astro-ph/9605140 [astro-ph].

- [41] P. Christian, S. Vitale, and A. Loeb, *Phys. Rev.* **D98**, 103022 (2018), arXiv:1802.02586 [astro-ph.HE].
- [42] T. Dent and C. Pankow, “Astrophysical Rates of Gravitational-Wave Compact Binary Sources in O3,” (2018), OpenLVEM Town Hall Meeting, Amsterdam, Netherlands.
- [43] E. D. Harstad, *A Targeted LIGO-Virgo Search for Gravitational Waves Associated with Gamma-Ray Bursts Using Low-Threshold Swift GRB Triggers*, Ph.D. thesis, Oregon U. (2013).
- [44] B. P. Abbott *et al.* (LIGO Scientific, Virgo), *Phys. Rev. Lett.* **121**, 231103 (2018), arXiv:1808.04771 [astro-ph.CO].
- [45] J. Veitch, V. Raymond, B. Farr, W. Farr, P. Graff, S. Vitale, B. Aylott, K. Blackburn, N. Christensen, M. Coughlin, W. Del Pozzo, F. Feroz, J. Gair, C.-J. Haster, V. Kalogera, T. Littenberg, I. Mandel, R. O’Shaughnessy, M. Pitkin, C. Rodriguez, C. Röver, T. Sidery, R. Smith, M. Van Der Sluys, A. Vecchio, W. Vousden, and L. Wade, *Phys. Rev. D* **91**, 042003 (2015), arXiv:1409.7215 [gr-qc].
- [46] C. Messick, K. Blackburn, P. Brady, P. Brockill, K. Cannon, R. Cariou, S. Caudill, S. J. Chamberlin, J. D. E. Creighton, R. Everett, C. Hanna, D. Keppel, R. N. Lang, T. G. F. Li, D. Meacher, A. Nielsen, C. Pankow, S. Privitera, H. Qi, S. Sachdev, L. Sadeghian, L. Singer, E. G. Thomas, L. Wade, M. Wade, A. Weinstein, and K. Wiesner, ArXiv e-prints (2016), arXiv:1604.04324 [astro-ph.IM].
- [47] S. Sachdev, S. Caudill, H. Fong, R. K. L. Lo, C. Messick, D. Mukherjee, R. Magee, L. Tsukada, K. Blackburn, P. Brady, P. Brockill, K. Cannon, S. J. Chamberlin, D. Chatterjee, J. D. E. Creighton, P. Godwin, A. Gupta, C. Hanna, S. Kapadia, R. N. Lang, T. G. F. Li, D. Meacher, A. Pace, S. Privitera, L. Sadeghian, L. Wade, M. Wade, A. Weinstein, and S. Liting Xiao, arXiv e-prints, arXiv:1901.08580 (2019), arXiv:1901.08580 [gr-qc].
- [48] S. A. Usman *et al.*, *Class. Quant. Grav.* **33**, 215004 (2016), arXiv:1508.02357 [gr-qc].
- [49] R. K. L. Lo, I. Hernandez, A. K. Y. Li, X. Liu, K. K. Y. Ng, J. D. E. Creighton, and T. G. F. Li, (In preparation) (2019).
- [50] D. Mukherjee *et al.*, (2018), arXiv:1812.05121 [astro-ph.IM].
- [51] B. Allen, W. G. Anderson, P. R. Brady, D. A. Brown, and J. D. E. Creighton, *Phys. Rev.* **D85**, 122006 (2012), arXiv:gr-qc/0509116 [gr-qc].
- [52] K. Cannon, C. Hanna, and D. Keppel, *Phys. Rev.* **D88**, 024025 (2013), arXiv:1209.0718 [gr-qc].
- [53] K. Cannon, C. Hanna, and J. Peoples, arXiv preprint arXiv:1504.04632 (2015).
- [54] B. P. Abbott *et al.* (LIGO Scientific, Virgo), *Phys. Rev.* **X6**, 041015 (2016), [erratum: *Phys. Rev.*X8,no.3,039903(2018)], arXiv:1606.04856 [gr-qc].
- [55] “O1 parameter estimation samples release,” .
- [56] H. K. Y. Fong, *From Simulations to Signals: Analyzing Gravitational Waves from Compact Binary Coalescences*, Ph.D. thesis, Department of Physics, University of Toronto (2018).
- [57] M. Vallisneri, J. Kanner, R. Williams, A. Weinstein, and B. Stephens, *Proceedings, 10th International LISA Symposium: Gainesville, Florida, USA, May 18-23, 2014*, *J. Phys. Conf. Ser.* **610**, 012021 (2015), arXiv:1410.4839 [gr-qc].